

RESEARCH

Open Access



Segmental strain for scar detection in acute myocardial infarcts and in follow-up exams using non-contrast CMR cine sequences

Malgorzata Polacin^{1,2*}, Mihaly Karolyi¹, Matthias Eberhard¹, Ioannis Matziris³, Hatem Alkadhi¹, Sebastian Kozerke² and Robert Manka^{1,2,3}

Abstract

Background: The purpose of the study was to investigate feasibility of infarct detection in segmental strain derived from non-contrast cardiac magnetic resonance (CMR) cine sequences in patients with acute myocardial infarction (AMI) and in follow-up (FU) exams.

Methods: 57 patients with AMI (mean age 61 ± 12 years, CMR 2.8 ± 2 days after infarction) were retrospectively included, FU exams were available in 32 patients (35 ± 14 days after first CMR). 43 patients with normal CMR (54 ± 11 years) served as controls. Dedicated software (Segment CMR, Medviso) was used to calculate global and segmental strain derived from cine sequences. Cine short axis stacks and segmental circumferential strain calculations of every patient and control were presented to two blinded readers in random order, who were advised to identify potentially infarcted segments, blinded to LGE and clinical information.

Results: Impaired global strain was measured in AMI patients compared to controls (global peak circumferential strain [GPCS] $p=0.01$; global peak longitudinal strain [GPLS] $p=0.04$; global peak radial strain [GPRS] $p=0.01$). In both imaging time points, mean segmental peak circumferential strain [SPCS] was impaired in infarcted tissue compared to remote segments (AMI: $p=0.03$, FU: $p=0.02$). SPCS values in infarcted segments were similar between AMI and FU ($p=0.8$). In SPCS calculations, 141 from 189 acutely infarcted segments were accurately detected (74.6%), visual evaluation of correlating cine images detected 43.4% infarcts. In FU, 80% infarcted segments (91/114 segments) were detected in SPCS and 51.8% by visual evaluation of correlating short axis cine images ($p=0.01$).

Conclusion: Segmental circumferential strain derived from routinely acquired native cine sequences detects nearly 75% of acute infarcts and 80% of infarcts in subacute follow-up CMR, significantly more than visual evaluation of correlating cine images alone. Acute infarcts may display only subtle impairment of wall motion and no obvious wall thinning, thus SPCS calculation might be helpful for scar detection in patients with acute infarcts, when LGE images are not available.

Keywords: Cardiac magnetic resonance, Acute myocardial infarction, Ischemic heart disease, Feature tracking

Background

Upon myocardial infarction, scar tissue is best visualized by cardiac magnetic resonance imaging (CMR) with late gadolinium enhancement (LGE) [1]. Intravenous application of gadolinium-based contrast agents is mandatory before acquiring LGE sequences. However, gadolinium

*Correspondence: Malgorzata.Polacin@usz.ch

¹ Institute of Diagnostic and Interventional Radiology, University Hospital Zurich, University of Zurich, Raemistrasse 100, 8091 Zurich, Switzerland
Full list of author information is available at the end of the article



© The Author(s) 2022. **Open Access** This article is licensed under a Creative Commons Attribution 4.0 International License, which permits use, sharing, adaptation, distribution and reproduction in any medium or format, as long as you give appropriate credit to the original author(s) and the source, provide a link to the Creative Commons licence, and indicate if changes were made. The images or other third party material in this article are included in the article's Creative Commons licence, unless indicated otherwise in a credit line to the material. If material is not included in the article's Creative Commons licence and your intended use is not permitted by statutory regulation or exceeds the permitted use, you will need to obtain permission directly from the copyright holder. To view a copy of this licence, visit <http://creativecommons.org/licenses/by/4.0/>. The Creative Commons Public Domain Dedication waiver (<http://creativecommons.org/publicdomain/zero/1.0/>) applies to the data made available in this article, unless otherwise stated in a credit line to the data.

should be used carefully in some patient groups, such as patients with severely reduced kidney function. Gadolinium-free options for the detection of ischemic myocardial scars are limited. One promising alternative is scar detection using regional myocardial deformation parameters [2, 3]. Myocardial deformation during cardiac contraction can be quantified by myocardial feature tracking (FT) based on routinely acquired, non-contrast cine sequences [4, 5]. Necrosis of myocytes after myocardial infarction with subsequent scar replacement disturbs mechanical properties of the myocardium with consecutively altered global and segmental strain [6]. Especially chronic myocardial scars with wall thinning and noticeable wall motion abnormality result in significant segmental strain impairment, which can be used to distinguish scar tissue from remote myocardium [2, 3, 7]. In contrast, acute infarcts might lack significant myocardial wall thinning and display less wall motion abnormalities in cine images. Therefore, the impact of acute and subacute infarcts on segmental strain needs to be further analyzed. In this study, global and segmental strain derived from non-contrast cine images was analyzed in patients with acute myocardial infarction (AMI) and in subacute follow-up (FU) exams and the practicability of using segmental strain for scar detection in both exams was investigated.

Methods

Study population

From July 2019 until December 2020 57 patients (15 female, mean age 61 ± 12 years) with AMI in CMR (imaging 2.8 ± 2 days [range 0–6 days] after reperfusion therapy) were retrospectively assessed. In those patients, CMR was performed to evaluate extent of infarction after revascularization [8]. Thirty-two out of 57 patients had a FU exam (35 ± 14 days, [range 20–86 days]). Patients with concomitant primary cardiomyopathies ($n = 2$) or non-diagnostic LGE images ($n = 3$) were not enrolled. Forty-three individuals (13 female, mean age 54 ± 11 years) with normal CMR examinations during the same time period were also retrospectively included. CMR referrals in the control group were exclusion of structural heart disease ($n = 16$) and exclusion of coronary artery disease ($n = 27$). Demographic characteristics of patients and controls are shown in Table 1a, b, respectively.

CMR data acquisition

CMR exams were acquired on a 1.5 T MR (Achieva, Philips Healthcare). Cine balanced steady-state free precession (SSFP) images in long-axis geometries (2-, 3- and 4-chamber view) and in short axis orientation covering the entire left ventricle (LV) (field of view: 350×350 mm²; matrix: 300×300 ; repetition time/echo

time: 3.0/1.5 ms; in-plane resolution 1.2×1.2 mm²; number of cardiac phases: 50; section thickness: 8 mm) were acquired for functional assessment of the LV. Edema-sensitive black-blood T2-weighted images with fat saturation in five short axis slices were acquired for visualization of myocardial edema [9]. Fifteen minutes after administration of gadolinium (0.2 mmol gadobutrol [Gadovist; Bayer Schering Pharma, Zurich, Switzerland] per kilogram body weight), LGE (inversion recovery gradient-echo sequence; field of view: 350×350 mm²; matrix: 234×234 ; repetition time/echo time: 7.4/4.4 ms; inversion time: 205–255 ms; flip angle: 20°; in-plane resolution: 1.5×1.5 mm²; section thickness: 8 mm) was performed in short axis and in 2-, 3- and 4 chamber view.

CMR data analysis

Strain analysis

Dedicated software (Segment v3.0 R7946, Medviso, Lund, Sweden) was used to calculate global and segmental strain derived from native cine sequences as previously described [3]. Duration of data loading, image registration, contouring of myocardial borders and strain calculation was $9 \text{ min } 58 \text{ s} \pm 35 \text{ s}$ (range 9 min 4 s–11 min 31 s) per patient or control, respectively. Blinded to patient information (patient or control) and to LGE images, all strain analyses were performed by one reader (reader A: 5 years of experience in cardiac imaging). Interobserver agreement was performed on 28 random cases by a second reader due to the semi-automatic nature of strain analyses (reader B: 2 years of experience in cardiac imaging, blinded to the results of reader A).

Infarct detection in circumferential strain calculations and in cine images

Reader A and B were advised to identify possibly infarcted segments in segmental circumferential strain calculations (right column of Fig. 1a, b) as well as in the corresponding short axis cine images, recognizing visual wall motion abnormalities (VWMA) as previously described [3]. Datasets of all patients (AMI and FU exams) and controls were mixed and presented in random order to both readers. Both readers were blinded to each other, to LGE/edema images (Fig. 1a, b, left column) and to clinical information.

Assessment of affected segments in LGE images and T2w

In a separate session, both readers had to define affected segments (short axis LGE, black-blood T2-weighted images with fat saturation), including classification of affected segments in LGE images in viable (below 50% infarcted wall thickness) or non-viable segments (more than 50% infarcted wall). Readers were blinded to clinical information and each other. Reference standard was the

Table 1 Demographic characteristics. a: Patients versus controls and b: AMI versus follow-up

	AMI n = 57	Controls n = 43	p values
<i>(a)</i>			
Demographics			
Sex (male/female)	42/15	30/13	–
Age (years)	61 ± 12	54 ± 11	0.2
BSA (m ²)	1.9 ± 0.4	1.8 ± 0.3	0.5
BMI	27 ± 5	25 ± 3	0.02
LV morphology			
LV-EDV (ml)	191 ± 23	171 ± 31	< 0.01
LV-ESV (ml)	81 ± 32	66 ± 21	< 0.01
LV-SV (ml)	83 ± 15	91 ± 15	0.02
LV-EF (%)	50 ± 8	59 ± 6	< 0.01
LV mass (g)	60 ± 14	51 ± 10	0.04
Global strain			
GPCS (%)	– 10.3 ± 3	– 19.9 ± 2	0.01
GPLS (%)	– 10.7 ± 5	– 18.9 ± 4	0.04
GPRS (%)	27.9 ± 5	39.8 ± 6	0.01
Affected coronary vessel			
RIVA			
Reperfused acute occlusion	28		
Reperfused acute-on-chronic stenosis	1		
Failed reperfusion	2		
Acute coronary dissection	2		
RCA—reperfused acute occlusion	13		
RCA—acute dissection	3		
LCX—reperfused acute occlusion	6		
LCX—failed reperfusion	2		
Myocardial infarcts			
Infarcted segments	189/896		
Viable (< 50% wall width infarcted)	3		
Non-viable (> 50% wall width infarcted)	186		
Scar burden (%)	23.4 ± 6		
Segments with myocardial edema only	27		
	AMI CMR	Follow-up CMR	p values
<i>(b)</i>			
n	32		
Sex (male/female)	23/9		
Age (years)	52 ± 7		
BSA (m ²)	1.9 ± 0.5		
BMI	27 ± 4		
LV morphology			
LV-EDV (ml)	172 ± 19	184 ± 27	0.2
LV-ESV (ml)	80 ± 29	86 ± 26	0.8
LV-SV (ml)	89 ± 18	72 ± 18	0.5
LV-EF (%)	47 ± 10	51 ± 8	0.2
LV mass (g)	60 ± 10	53 ± 8	0.6
Global strain			
GPCS (%)	– 10.6 ± 2	– 9.5 ± 3	0.7

Table 1 (continued)

	AMI CMR	Follow-up CMR	<i>p</i> values
GPLS (%)	− 10.2 ± 5	− 10.9 ± 5	0.8
GPRS (%)	26.8 ± 6	29.8 ± 4	0.2
Myocardial infarcts			
Infarcted segments	118/512	118/512	
Viable (< 50% wall width infarcted)	1	16	0.02
Non-viable (> 50% wall width infarcted)	117	102	0.5
Scar burden (%)	25.1 ± 5	20.7 ± 4	0.6
Segments with myocardial edema only	10	–	–
Patients with infarcts detected in SPCS ^a	32/32	31/32	–

BSA body surface area, BMI body mass index, LVEDV left ventricular end-diastolic volume, LVESV left ventricular end-systolic volume, LVSV left ventricular stroke volume, LVEF left ventricular ejection fraction, GPCS/GPLs/GPRS global circumferential/longitudinal/radial strain

^a Patients with infarcts in LGE served as gold standard

existing corresponding CMR report, revised by a cardiologist with over 15 years of experience in CMR (EACVI level III certified). Ventricular volumes and function were calculated using IntelliSpace Portal, performed by reader A (Philips, Version 8.0.3; Table 1a, b).

Statistical analyses

Statistics were performed using commercially available software (IBM SPSS Statistics, release 25.0; SPSS, Armonk, NY). Categorical data are expressed as numbers or percentages and quantitative data are expressed as means ± standard deviations. Normal distribution was tested by the Kolmogorov–Smirnov test. Two-tailed paired *t* tests or Wilcoxon signed rank were used to compare global and segmental strain values as well as to compare infarcted segments found in LGE, circumferential strain calculations and by visual wall motion assessment. Interobserver agreement was investigated using the intraclass correlation coefficient (ICC). ICC = 0.50–0.75 was considered moderate, ICC = 0.75–0.9 was considered good and ICC > 0.9 was considered excellent agreement [10]. Receiver operating characteristics (ROC) were calculated to determine the cut-offs of segmental strain values and area under the curve (AUC) for segmental strain (SPCS, SPRS and SPLS) in order to differentiate infarcted from remote myocardium. Statistical significance was supposed at a *p* value below 0.05.

Results

LGE and edema

In patients with acute infarction, 189 out of 896 segments showed LGE (21.1%) and myocardial edema. Myocardial edema was also detected in 27 segments without LGE. Mean scar burden per patient was 23.4% ± 6 (range 8–59%), the average amount of infarcted segments

per patient was 3.7 (range: 2–9 segments) and most infarcted segments were considered non-viable (186/189) (Table 1a).

In the subgroup of patients with follow-up exams 118 out of 512 segments showed LGE (23%). Mean scar burden at acute imaging timepoint was 25.1% ± 5 per patient (range 12–56%) with mostly non-viable scars (117/118), further 10 segments had myocardial edema without concomitant LGE. Scar burden decreased in follow-up exams (20.7 ± 4, range 5–48%) and 15 segments were reclassified from non-viable in AMI exams to viable in FU (Table 1b). No LGE was found in the control group.

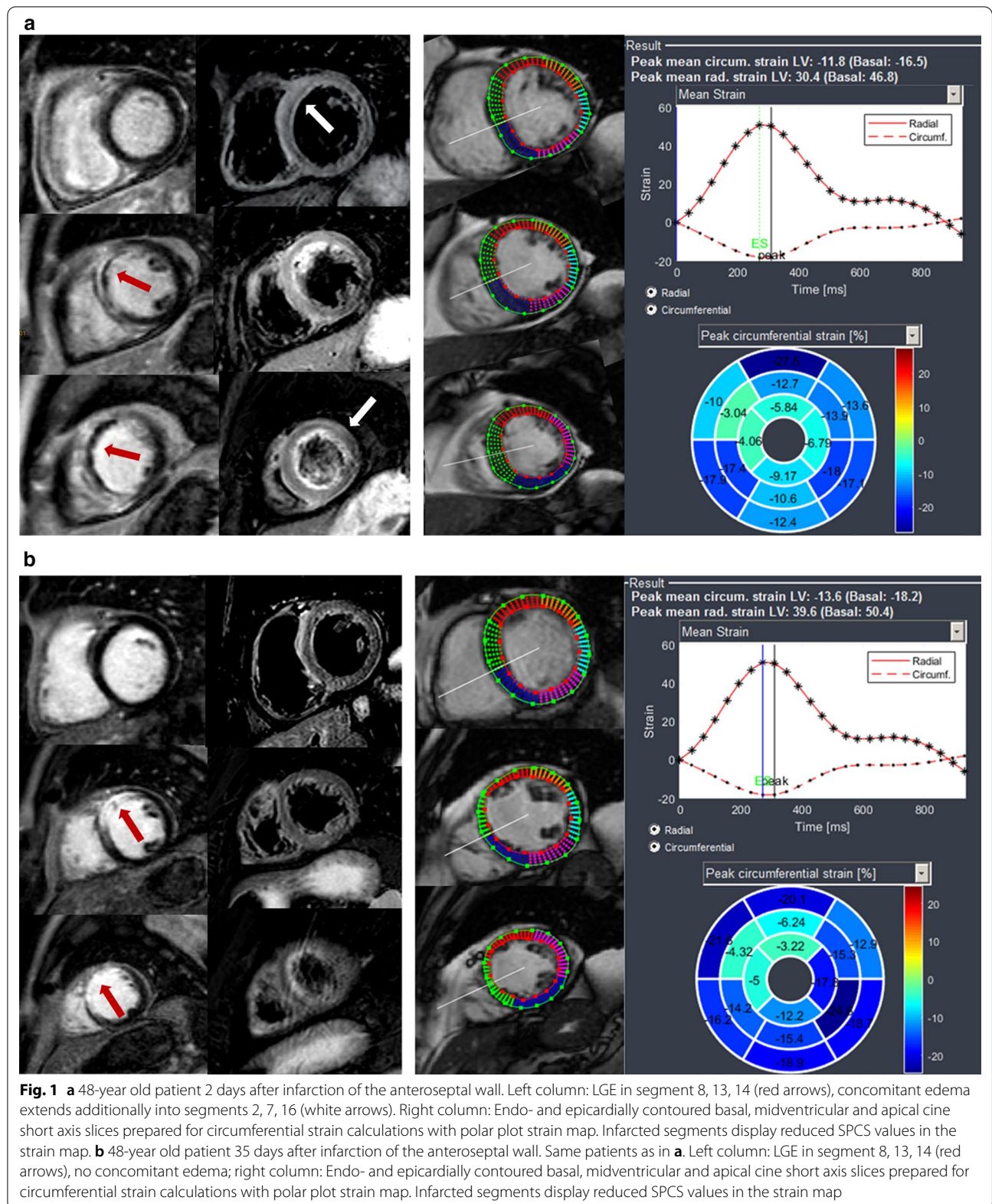
Global strain

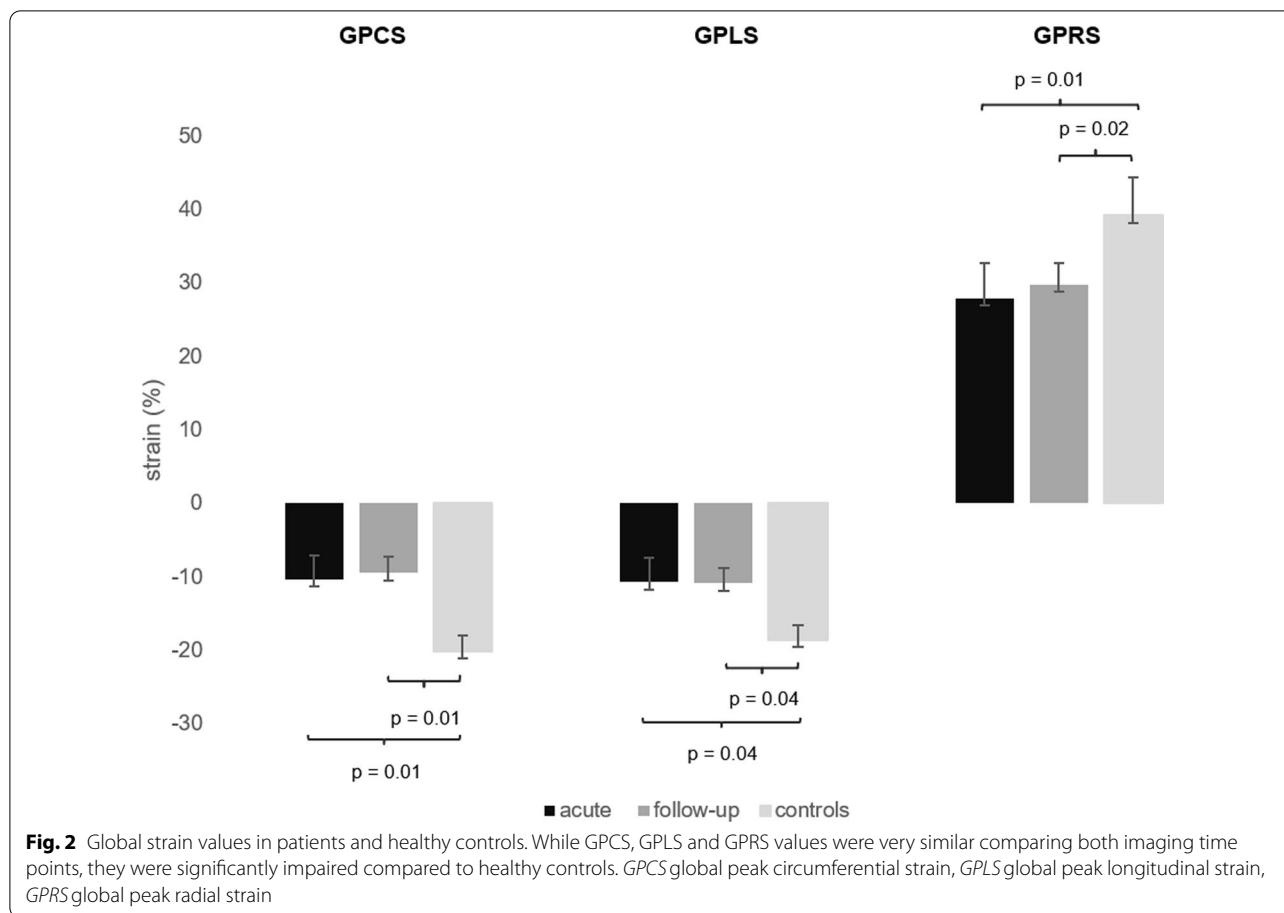
In patients, mean global strain was impaired compared to controls (global peak circumferential strain [GPCS]: − 10.3% ± 3 vs. − 19.9% ± 2, *p* = 0.01; global peak longitudinal strain [GPLS]: − 10.7% ± 5 vs. − 18.9% ± 4, *p* = 0.04; global peak radial strain [GPRS]: 27.9% ± 5 vs. 39.8% ± 6; *p* = 0.01, Fig. 2). In the subgroup with follow-up CMR, similar mean global strain values were measured between both time points (GPCS: − 10.6% ± 2 vs. − 9.5% ± 3, *p* = 0.7; GPLS − 10.2% ± 5 vs. − 10.9% ± 5, *p* = 0.8; GPRS 26.8% ± 6 vs. 29.8% ± 4; *p* = 0.2; Fig. 2).

Segmental strain

Segmental strain in patients with AMI

In patients with AMI, mean segmental peak circumferential strain (SPCS) was markedly impaired in infarcted segments compared to mean SPCS of healthy myocardium (− 2% ± 1 vs. − 10.5% ± 1, *p* = 0.03, Fig. 3), interobserver agreement was excellent (Table 2). Mean segmental peak longitudinal strain (SPLS) and mean segmental peak radial strain (SPRS) in infarcted segments were mildly impaired (SPLS − 6.5% ± 8 and SPRS





15.9% ± 7) compared to SPLS and SPRS of remote myocardium (SPLS - 11.8% ± 5 and SPRS 23.4% ± 7, $p=0.7$ and 0.5) (Fig. 3). From 189 segments with LGE, 141 could be identified in cine based segmental circumferential strain calculations (74.6%; ICC 0.869, 95% CI 0.811–0.908). Moreover, both readers detected all patients with scars in strain calculations, the “missed” 48 segments belonged to patients, that were already diagnosed with at least one infarcted segment. 15 segments were assumed “infarcted” in circumferential strain calculations without displaying LGE, all those segments had myocardial edema. Visual assessment of wall motion abnormalities (VWMA) in cine images revealed 82 infarcted segments out of 189 (43.4%; ICC 0.789, 95% CI 0.729–0.821; Fig. 4). No normal segments (without edema and LGE) in patients nor segments in controls were assumed infarcted by VWMA or circumferential strain calculations.

Segmental strain in follow-up CMR

In FU exams, mean SPCS and SPRS were also significantly impaired in infarcted segments compared to SPCS and SPRS of remote myocardium (SPCS - 2.4% ± 2 vs. - 13.4% ± 2, $p=0.02$; SPRS 16.7% ± 4 vs. 32.4% ± 3,

$p=0.02$; Fig. 3) with excellent interobserver agreement (Table 2). Viable scars had only subtle SPCS impairment (SPCSviable - 8.1% ± 4 vs. SPCS - 2.4% ± 2, $p=0.1$). Direct comparison between imaging in the acute setting and in follow-up CMR revealed no significant differences in segmental strain values between infarcted segments and remote myocardium, however, a tendency towards lower segmental circumferential strain of remote myocardium in the acute subgroup was noticeable (AMI - 10.6% ± 1 vs. FU exam - 12.9% ± 2, $p=0.07$; Fig. 3).

ROC analyses were performed for SPCS, SPRS and SPLS to detect the optimal cut-off values for discrimination of infarcted segments and remote myocardium; infarcts visible in LGE were considered reference standard (Fig. 5). A SPCS value below - 5.9% was considered infarcted (sensitivity of 86.2%, specificity of 83.5%, AUC 0.89 [95% CI 0.878–0.923, $p<0.05$]). The cut-off value for SPRS was 20.2% (sensitivity of 77.5%, specificity of 77.9%, AUC 0.78 [95% CI 0.718–0.814, $p<0.05$]) and for SPLS - 6.6% (sensitivity of 60.4%, specificity of 72.9%, AUC 0.66 [95% CI 0.598–0.715, $p<0.05$]).

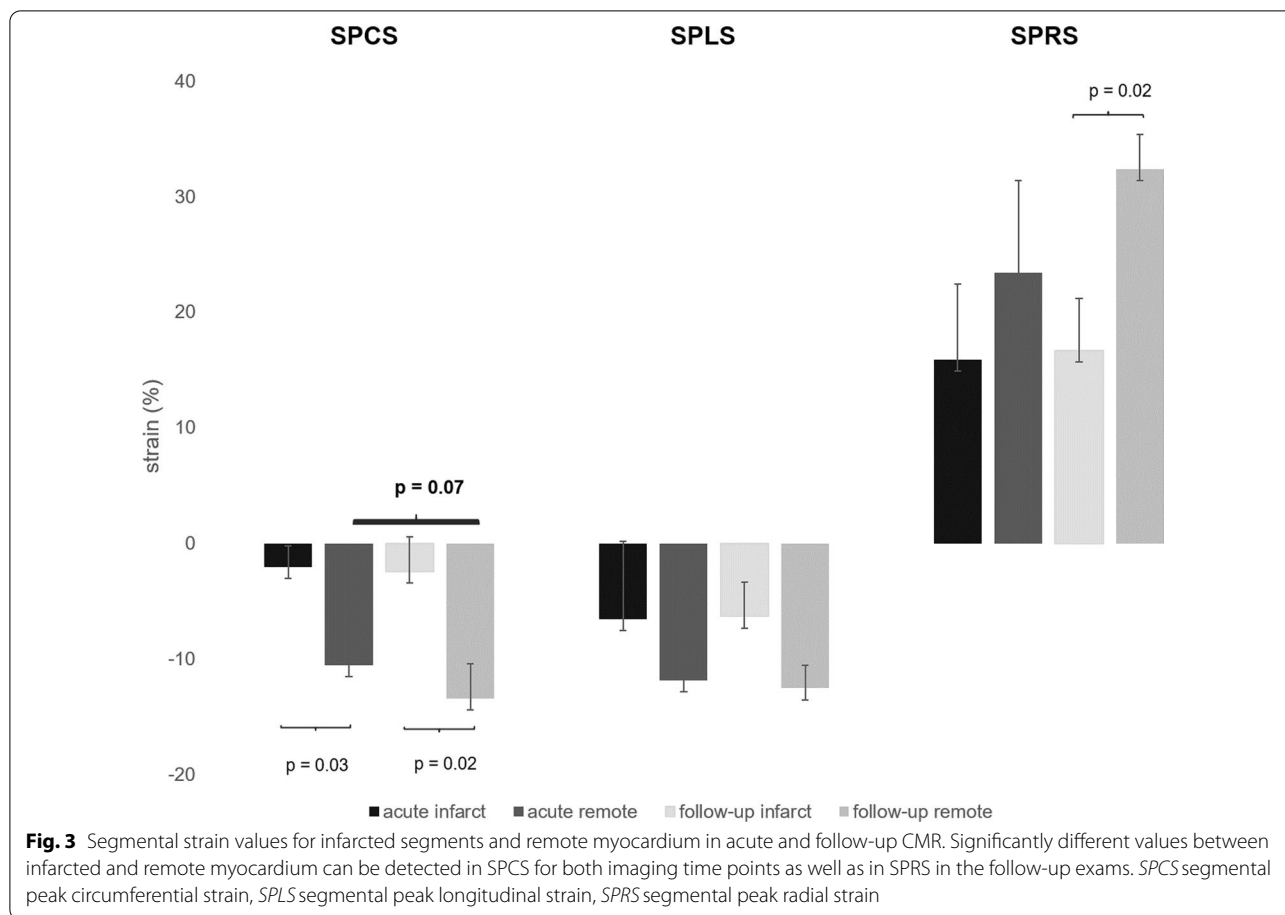


Table 2 Interobserver agreement

	ICC acute	ICC follow up
Global strain		
GPCS	0.902 [95% CI 0.878–0.930]	0.916 [95% CI 0.882–0.941]
GPLS	0.850 [95% CI 0.817–0.879]	0.878 [95% CI 0.804–0.929]
GPRS	0.893 [95% CI 0.851–0.939]	0.897 [95% CI 0.878–0.947]
Segmental strain		
SPCS	0.899 [95% CI 0.862–0.922]	0.903 [95% CI 0.869–0.934]
SPLS	0.732 [95% CI 0.711–0.749]	0.719 [95% CI 0.701–0.747]
SPRS	0.804 [95% CI 0.793–0.869]	0.817 [95% CI 0.797–0.902]

GPCS/GPLG/GPRS global circumferential/longitudinal/radial strain, SPCS/SPLS/SPRS segmental circumferential/longitudinal/radial strain, ICC intraclass correlation coefficient

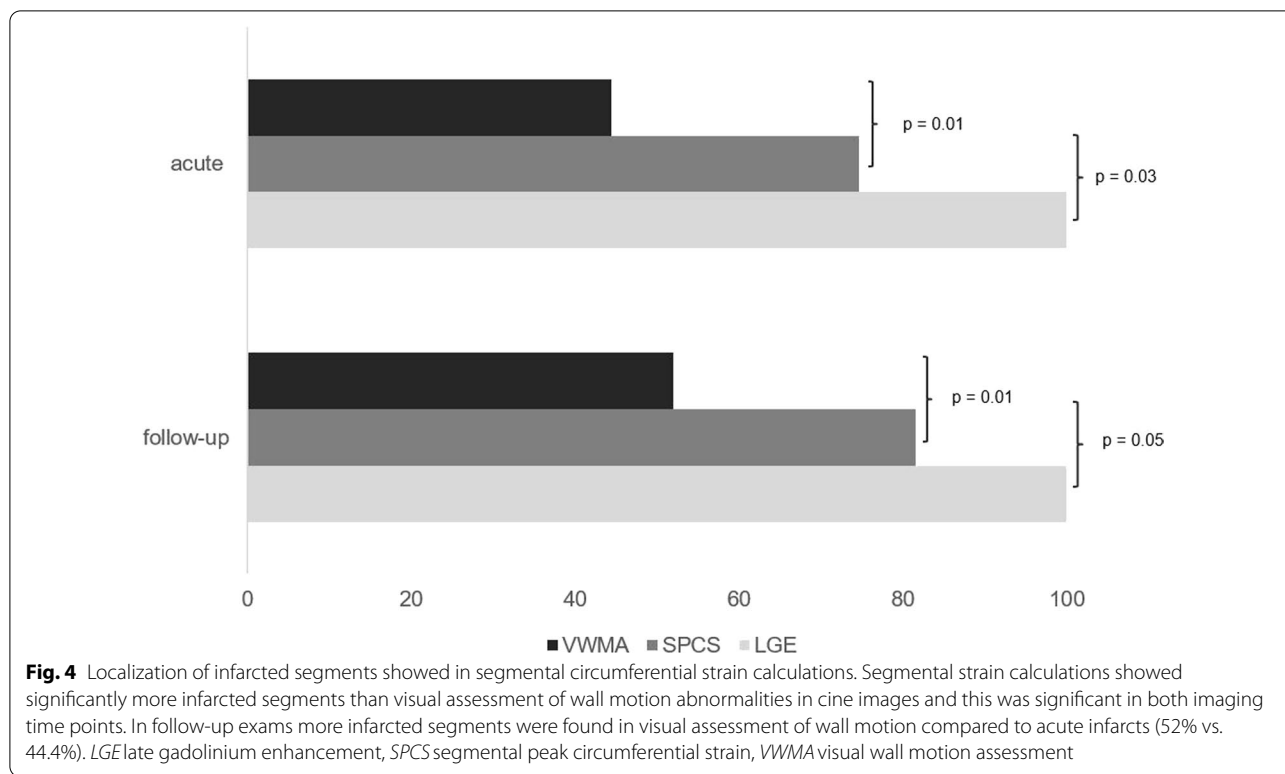
Evaluation of segmental circumferential strain calculations detected 91 out of 114 infarcted segments (80%; ICC 0.865, 95% CI 0.802–0.908), detection of VWMA in cine sequences revealed 59 segments (51.8%; ICC 0.802, 95% CI 0.759–0.831; Fig. 4). Both readers missed one patient with subtle viable scar (one

infarcted segment) in segmental circumferential strain calculation.

Discussion

This study analyzed the feasibility of using segmental strain for scar detection in patients with acute and sub-acute myocardial infarcts. Segmental circumferential strain calculations based on native cine images detected all patients with AMI and 80% of infarcted segments in subacute follow-up exams.

In the clinical setting, established alternatives for scar detection in native CMR sequences are limited. With native T1 mapping, scar and remote myocardium can be differentiated due to different tissue relaxation times [11, 12]. However, additional mapping sequences need to be acquired and in order to achieve accurate measurements standardized parameters for healthy myocardium need to be defined separately for every scanner. Moreover, while acute infarcts can be reliably detected in native T1 maps, T1 values of infarcted areas normalize after acute infarction with resulting lower specificity for chronic infarcts [13]. Some artificial intelligence-based techniques successfully detected scar tissue in



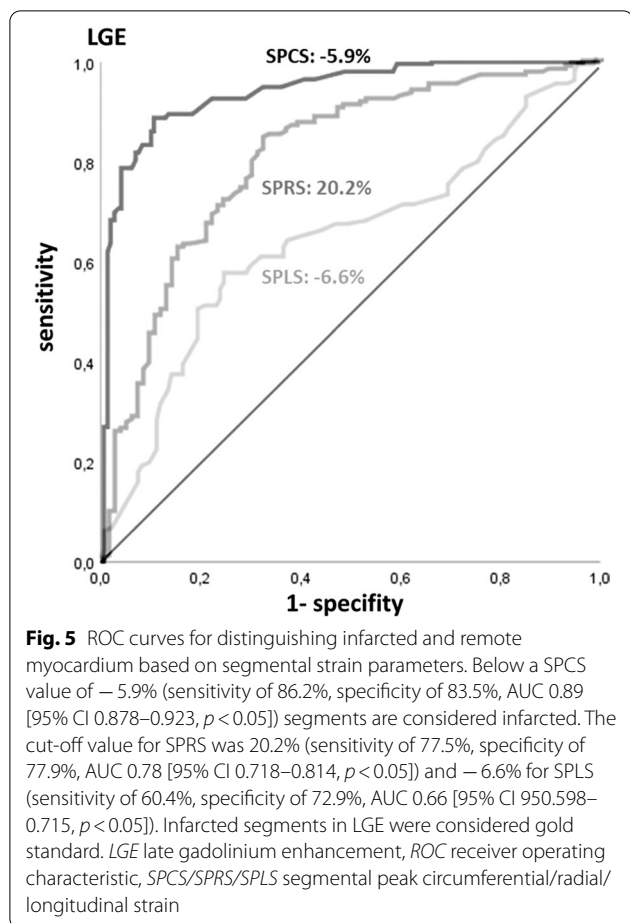
non-contrast cine CMR sequences [14, 15], but these methods are mostly still in a proof-of-concept stage and are not yet practicable in clinical use.

Myocardial feature tracking (FT) was introduced as a novel technique for myocardial strain quantification based on routinely acquired cine sequences. Infarcted tissue leads to altered global and segmental myocardial strain due to reduced contractility of fibroblasts, that gradually replace necrotic myocardium after myocardial infarction [6]. Impairment of global strain in patients with acute and chronic infarcts has been reported by various studies [16, 17]. Accordingly, GPLS, GPRS and especially GPCS was impeded in our patient cohort compared to healthy controls. Studies analyzing segmental strain in patients with infarcts in the last decade revealed heterogenous results, in particular problems with accuracy and reproducibility of segmental strain values have been reported [18]. Newer algorithms for strain quantification based on non-rigid algorithm for image registration and segmentation with tracking of the whole image content—instead of tracking myocardial borders only—seem to accurately identify scarred myocardium in segmental circumferential strain [19, 20].

Chronic scars with wall motion abnormalities and myocardial wall thinning lead to severe impairment of regional deformation parameters in contrast to healthy

tissue, allowing distinction of remote and infarcted segments in regional strain measurements [2, 7].

However, the impact of acute infarcts on segmental strain in native cine images has not yet been sufficiently investigated. In contrast to chronic infarcts, which may be visible with the bare eye in cine images due to wall thinning or dyskinesia and are characterized by replacement fibrosis, acutely infarcted myocardium with its various pathophysiologic processes including necrosis and edema mostly lacks wall thinning and has often only subtle wall motion abnormality [21, 22]. Therefore, possible strain impairment in acute infarcts is apparently based on different mechanisms compared to strain impairment in chronic scars. Nevertheless, similar to chronic infarcts, regional mechanical impairment of acutely infarcted myocardium was best reflected in circumferential strain calculations [23]. In our patient cohort, mean SPCS in infarcted tissue was significantly impaired compared to SPCS of remote myocardium and this was observed in both acute imaging as well as in subacute follow-up CMRs. Comparing both exams, infarcted tissue showed similar mean SPCS values, remote myocardium on the other hand showed slightly more impairment in the acute imaging timepoint. Further analyses revealed that edematous segments adjacent to infarcts caused strain impairment, suggesting influence of myocardial edema on segmental circumferential strain. Accordingly,



false positive classification of edematous segments as “infarcted” by both readers was observed in the acute timepoint. After edema subsided in follow-up exams, no false positive results were noticed.

Similar to chronic infarcts, infarcted segments could be distinguished from healthy myocardium with high sensitivity and specificity below a calculated threshold in SPCS calculations, while sensitivity and specificity was markedly lower for corresponding thresholds in SPRS and SPLS.

Direct comparison of wall motion and segmental circumferential strain calculations of every patient in a blinded dataset revealed markedly more infarcted segments in SPCS calculations than by analyzing cine images only and this was true for the acute timepoint (74.6% vs. 43.4%) as well as in follow-up exams (80% vs. 52%). The higher amount of infarcted segments detected by VWMA in follow-up exams could be explained with the incremental myocardial thinning weeks after infarction.

Perfect sensitivity for the detection of patients with AMI was observed in SPCS calculations, where missed infarcted segments belonged to patients already classified

as “patient with infarction” by the readers. In follow-up exams, when LGE burden subsided, some scarred segments were reclassified from non-viable to viable scars. Viable scars showed lesser SPCS impairment than non-viable infarcts and in fact one patient with a small viable scar was classified as “patient with no infarction” in SPCS calculations by both readers. SPCS impairment mainly correlates with damage of circumferentially orientated myocardial fibers, that lay below the superficial subendocardial fibers of the LV myocardium [24, 25]. In viable scars, deeper lying circumferential fibers are probably not enough affected to cause significant SPCS impairment. This is a relevant limitation of this study, since most infarcts in our patient cohort were non-viable. Furthermore, regional deformation parameters detected by segmental strain are influenced by various factors and are not specific for ischemic tissue damage. Further studies are needed to analyse segmental strain in patients with infarcts and concomitant cardiac diseases that are known to influence global strain like cardiomyopathies or storage disease [26, 27]. Moreover, temporary cardiac conditions like myocardial hibernation or stunning or even benign anatomical variants like a left ventricular diverticulum with potential impact on segmental strain needs to be examined, preferably in a prospective setting with a larger patient cohort. In this retrospective study with initially 57 patients, follow-up exams were available in only 32 individuals. The mean interval of 5 weeks between initial imaging and follow-up CMR is presumably not long enough to measure remodelling, because of still ongoing pathophysiologic processes and distant time points should be investigated for that matter in further studies. In addition, segmental circumferential strain calculations use the 16-segment model and apical infarction (segment 17) cannot be detected in SPCS calculations.

Ultimately, strain measurements were performed with only one software. Recent studies show, that strain values are not interchangeable between different vendors, thus vendor-specific threshold values need to be defined for infarcted and remote myocardium [20].

Conclusion

Segmental circumferential strain derived from routinely acquired non-contrast cine sequences detects nearly 75% of acute infarcts and 80% of infarcts in subacute follow-up CMR, significantly more than visual evaluation of cine images alone. Especially in acute infarcts, where wall motion abnormalities may be subtle and wall thinning is not yet present, this technique may aid infarct detection in patients with ischemic heart disease, who cannot receive or reject gadolinium application or when LGE images are non-diagnostic. However, since strain impairment is not specific for ischemic tissue damage, further studies

are needed to investigate if this technique can be used in patients with concomitant cardiac conditions (e.g. cardiomyopathies) where global strain parameters may be altered.

Abbreviations

AMI: Acute myocardial infarction; AUC: Area under the curve; CMR: Cardiac magnetic resonance; FT: Feature tracking; FU: Follow-up (exam); GPCS: Global peak circumferential strain; GPLS: Global peak longitudinal strain; GPRS: Global peak radial strain; ICC: Intraclass correlation coefficient; i.v.: Intravenous; LGE: Late gadolinium enhancement; LV: Left ventricle/left-ventricular; LVEDV: Left ventricular end-diastolic volume; LVEF: Left ventricular ejection fraction; LVESV: Left ventricular end-systolic volume; LVSF: Left ventricular stroke volume; ms: Milliseconds; min: Minute(s); ROC: Receiver operating characteristics; s: Seconds; SPCS: Segmental peak circumferential strain; SPLS: Segmental peak longitudinal strain; SPRS: Segmental peak radial strain; SSFP: Steady-state free precession; T: Tesla; VWMA: Visual wall motion abnormality.

Acknowledgements

Not applicable.

Author contributions

M.P. and R.M. designed the study. M.P., M.K., M.E. and I.M. provided patient data and images. M.P. and M.K. performed data analysis. M.P. wrote the manuscript. M.E., H.A., S.K. and R.M. proofread the manuscript. All authors read and approved the final manuscript.

Funding

M.P. was financially supported by a grant from the Promedica Foundation.

Availability of data and materials

The datasets generated and analysed during this study are not publicly available due to their patient referable character, thereby compromising individual privacy, but are available from the corresponding author on reasonable request.

Declarations

Ethics approval and consent to participate

This retrospective study was conducted in accordance to the Declaration of Helsinki and its later amendments and the institutional review board approved this retrospective study (Cantonal ethics commission, Canton Zurich, BASEC-Nr. 2019-00808; committee's reference number: not applicable). All participants gave written informed consent.

Consent for publication

Not applicable.

Competing interests

The authors declare they have no competing interests.

Author details

¹Institute of Diagnostic and Interventional Radiology, University Hospital Zurich, University of Zurich, Raemistrasse 100, 8091 Zurich, Switzerland. ²Institute for Biomedical Engineering, University and ETH Zurich, Gloriastrasse 35, 8092 Zurich, Switzerland. ³Department of Cardiology, University Heart Center, University Hospital Zurich, University of Zurich, Raemistrasse 100, 8091 Zurich, Switzerland.

Received: 4 July 2021 Accepted: 3 May 2022

Published online: 18 May 2022

References

- Treibel TA, White SK, Moon JC. Myocardial tissue characterization: histological and pathophysiological correlation. *Curr Cardiovasc Imaging Rep.* 2014;7:1–9. <https://doi.org/10.1007/s12410-013-9254-9>.
- Tantawy SW, Mohammad SA, Osman AM, El Mozy W, Ibrahim AS. Strain analysis using feature tracking cardiac magnetic resonance (FT-CMR) in the assessment of myocardial viability in chronic ischemic patients. *Int J Cardiovasc Imaging.* 2020. <https://doi.org/10.1007/s10554-020-02018-w>.
- Polacin M, Karolyi M, Eberhard M, Gotschy A, Baessler B, Alkadhi H, et al. Segmental strain analysis for the detection of chronic ischemic scars in non-contrast cardiac MRI cine images. *Sci Rep.* 2021;11:1–11. <https://doi.org/10.1038/s41598-021-90283-7>.
- Claus P, Omar AMS, Pedrizzetti G, Sengupta PP, Nagel E. Tissue tracking technology for assessing cardiac mechanics: principles, normal values, and clinical applications. *JACC Cardiovasc Imaging.* 2015. <https://doi.org/10.1016/j.jcmg.2015.11.001>.
- Pedrizzetti G, Claus P, Kilner PJ, Nagel E. Principles of cardiovascular magnetic resonance feature tracking and echocardiographic speckle tracking for informed clinical use. *J Cardiovasc Magn Reson.* 2016. <https://doi.org/10.1186/s12968-016-0269-7>.
- Richardson WJ, Clarke SA, Alexander Quinn T, Holmes JW. Physiological implications of myocardial scar structure. *Compr Physiol.* 2015. <https://doi.org/10.1002/cphy.c140067>.
- Zou Q, Zheng T, Zhou SL, Tang XP, Li SH, Zhou W, et al. Quantitative evaluation of myocardial strain after myocardial infarction with cardiovascular magnetic resonance tissue-tracking imaging. *Int Heart J.* 2020;61:429–36. <https://doi.org/10.1536/ihj.19-384>.
- Bulluck H, Dharmakumar R, Arai AE, Berry C, Hausenloy DJ. Cardiovascular magnetic resonance in acute ST-segment-elevation myocardial infarction: recent advances, controversies, and future directions. *Circulation.* 2018;137:1949–64. <https://doi.org/10.1161/CIRCULATIONAHA.117.030693>.
- Simonetti OP, Finn JP, White RD, Laub G, Henry DA. "Black blood" T2-weighted inversion-recovery MR imaging of the heart. *Radiology.* 1996. <https://doi.org/10.1148/radiology.199.1.8633172>.
- Koo TK, Li MY. A guideline of selecting and reporting intraclass correlation coefficients for reliability research. *J Chiropr Med.* 2016. <https://doi.org/10.1016/j.jcm.2016.02.012>.
- Taylor AJ, Salerno M, Dharmakumar R, Jerosch-Herold M. T1 mapping basic techniques and clinical applications. *JACC Cardiovasc Imaging.* 2016. <https://doi.org/10.1016/j.jcmg.2015.11.005>.
- Thongsongsang R, Songsangjinda T, Tanapibunpon P, Krittayaphong R. Native T1 mapping and extracellular volume fraction for differentiation of myocardial diseases from normal CMR controls in routine clinical practice. *BMC Cardiovasc Disord.* 2021;21:1–17. <https://doi.org/10.1186/s12872-021-02086-3>.
- O H-Ici D, Jeuthe S, Al-Wakeel N, Berger F, Kuehne T, Kozerke S, et al. T1 mapping in ischaemic heart disease. *Eur Heart J Cardiovasc Imaging.* 2014. <https://doi.org/10.1093/ehjci/jeu024>.
- Zhang N, Yang G, Gao Z, Xu C, Zhang Y, Shi R, et al. Deep learning for diagnosis of chronic myocardial infarction on nonenhanced cardiac cine MRI. *Radiology.* 2019. <https://doi.org/10.1148/radiol.2019182304>.
- Baessler B, Mannil M, Oebel S, Maintz D, Alkadhi H, Manka R. Subacute and chronic left ventricular myocardial scar: accuracy of texture analysis on nonenhanced cine MR images. *Radiology.* 2018. <https://doi.org/10.1148/radiol.2017170213>.
- Reindl M, Tiller C, Holzknacht M, Lechner I, Beck A, Plappert D, et al. Prognostic implications of global longitudinal strain by feature-tracking cardiac magnetic resonance in ST-elevation myocardial infarction. *Circ Cardiovasc Imaging.* 2019. <https://doi.org/10.1161/CIRCIMAGING.119.009404>.
- Nucifora G, Muser D, Tioni C, Shah R, Selvanayagam JB. Prognostic value of myocardial deformation imaging by cardiac magnetic resonance feature-tracking in patients with a first ST-segment elevation myocardial infarction. *Int J Cardiol.* 2018. <https://doi.org/10.1016/j.ijcard.2018.05.082>.
- Ogawa R, Kido T, Nakamura M, Kido T, Kurata A, Miyagawa M, et al. Diagnostic capability of feature-tracking cardiovascular magnetic resonance to detect infarcted segments: a comparison with tagged magnetic resonance and wall thickening analysis. *Clin Radiol.* 2017. <https://doi.org/10.1016/j.crad.2017.05.010>.
- Morais P, Marchi A, Bogaert JA, Dresselaers T, Heyde B, D'Hooge J, et al. Cardiovascular magnetic resonance myocardial feature tracking using a non-rigid, elastic image registration algorithm: assessment of variability in a real-life clinical setting. *J Cardiovasc Magn Reson.* 2017. <https://doi.org/10.1186/s12968-017-0333-y>.

20. Dobrovie M, Barreiro-Pérez M, Curione D, Symons R, Claus P, Voigt JU, et al. Inter-vendor reproducibility and accuracy of segmental left ventricular strain measurements using CMR feature tracking. *Eur Radiol*. 2019;29:6846–57. <https://doi.org/10.1007/s00330-019-06315-4>.
21. Masci PG, Bogaert J. Post myocardial infarction of the left ventricle: the course ahead seen by cardiac MRI. *Cardiovasc Diagn Ther*. 2012. <https://doi.org/10.3978/j.issn.2223-3652.2012.04.06>.
22. Rajiah P, Desai MY, Kwon D, Flamm SD. MR imaging of myocardial infarction. *Radiographics*. 2013;33:1383–412. <https://doi.org/10.1148/rg.335125722>.
23. Wamil M, Borlotti A, Liu D, Briosa e Gala A, Bracco A, Alkhalil M, et al. Combined T1-mapping and tissue tracking analysis predicts severity of ischemic injury following acute STEMI—an Oxford Acute Myocardial Infarction (OxAMI) study. *Int J Cardiovasc Imaging*. 2019. <https://doi.org/10.1007/s10554-019-01542-8>.
24. Ho SY. Anatomy and myoarchitecture of the left ventricular wall in normal and in disease. *Eur J Echocardiogr*. 2009;10:3–7. <https://doi.org/10.1093/ejehocard/jep159>.
25. Scatteia A, Baritussio A, Bucciarelli-Ducci C. Strain imaging using cardiac magnetic resonance. *Heart Fail Rev*. 2017;22:465–76. <https://doi.org/10.1007/s10741-017-9621-8>.
26. Pu C, Fei J, Lv S, Wu Y, He C, Guo D, et al. Global circumferential strain by cardiac magnetic resonance tissue tracking associated with ventricular arrhythmias in hypertrophic cardiomyopathy patients. *Front Cardiovasc Med*. 2021;8:1–8. <https://doi.org/10.3389/fcvm.2021.670361>.
27. Pandey T, Alapati S, Wadhwa V, Edupuganti MM, Gurram P, Lensing S, et al. Evaluation of myocardial strain in patients with amyloidosis using cardiac magnetic resonance feature tracking. *Curr Probl Diagn Radiol*. 2017;46:288–94. <https://doi.org/10.1067/j.cpradiol.2016.11.008>.

Publisher's Note

Springer Nature remains neutral with regard to jurisdictional claims in published maps and institutional affiliations.

Ready to submit your research? Choose BMC and benefit from:

- fast, convenient online submission
- thorough peer review by experienced researchers in your field
- rapid publication on acceptance
- support for research data, including large and complex data types
- gold Open Access which fosters wider collaboration and increased citations
- maximum visibility for your research: over 100M website views per year

At BMC, research is always in progress.

Learn more biomedcentral.com/submissions

